Metal-Ion-Mediated Allosteric Triggering of Yeast Pyruvate Kinase 2. A Multidimensional Thermodynamic Linked-Function Analysis†

Andrew D. Mesecar‡,§ and Thomas Nowak*

Department of Chemistry and Biochemistry, University of Notre Dame, Notre Dame, Indiana 46556

Received November 20, 1996; Revised Manuscript Received March 5, 1997⊗

ABSTRACT: A role has been proposed for the free divalent metal in triggering the allosteric responses of yeast pyruvate kinase based upon a kinetic linked-function analysis [Mesecar, A. D., & Nowak, T. (1997a) (preceding paper in this series)]. The major conclusion from the analysis is that the allosteric activator, fructose 1,6-diphosphate (FDP), does not directly communicate with the substrate, phosphoenolpyruvate (PEP), at the active site of the enzyme: it is Mn^{2+} that mediates the allosteric communication between the PEP and FDP sites in an allosteric relay mechanism. Assumptions were necessary to treat kinetic parameters as thermodynamic parameters, and the presence of the substrate ADP was necessary for the kinetic analysis. In this study, the influence of FDP on the interactions of PEP and Mn^{2+} and the influence of PEP and Mn^{2+} on the interaction of FDP with YPK were measured, where possible, by direct binding methods in the absence of ADP. Direct binding data were then subjected to a thermodynamic linked-function analysis for a heterotropic, three ligand coupled system in order to ascertain the two and three ligand coupling free energies. The two ligand coupling free energies ΔG_{Mn-PEP}, ΔG_{Mn-FDP}, and $\Delta G_{PEP-FDP}$ are −3.88, −1.09, and −0.22 kcal/mol, respectively. These values indicate that positive, heterotropic interactions exist between each of these ligand pairs. The three ligand coupling free energy term, $\Delta G_{Mn-PEP-FDP}$, indicates that simultaneous binding of Mn^{2+}, PEP, and FDP is considerably favored over the sum of their independent binding free energies by −6.6 kcal/mol. These results demonstrate the key role of the metal in the modulation of ligand binding and are consistent with the values and the relationships of the kinetic parameters obtained from the kinetic linked-function analysis.

Pyruvate kinase from the yeast *Saccharomyces cerevisiae* is an interesting and complex regulatory enzyme that is involved in a key energy producing step in glycolysis. The enzyme catalyzes the essentially irreversible transfer of a phosphoryl group from phosphoenolpyruvate (PEP)[1] to ADP to form pyruvate and ATP:

$$H^+ + PEP + M(II)ADP \xrightleftharpoons{M(I),\ M(II)} Pyruvate + M(II)ATP$$

The reaction requires both monovalent and divalent cations, normally K^+, and Mg^{2+} or Mn^{2+}. Yeast pyruvate kinase (YPK) is subject to allosteric regulation by a number of physiological effectors including PEP, ATP, H^+, Mn^{2+}, K^+, and fructose 1,6-diphosphate (FDP). A number of the interactions between these ligands with the enzyme are coupled and complex and involve both homotropic and heterotropic cooperativity (Mesecar & Nowak, 1997a). The response of YPK to the binding of the substrate ADP is hyperbolic and considered simple since homotropic cooperativity has not been observed under a variety of conditions. Because ADP generally does not exhibit cooperative interactions with pyruvate kinase, it is usually not included in cooperative ligand binding models for pyruvate kinases. In our steady-state kinetic analysis, we found it necessary to consider free ADP and its interactions with YPK to explain deviations observed in our kinetic data for cooperative interactions with YPK. The work described herein circumvents the problems of including ADP in our analyses by excluding it from the complexes formed.

A recent quantitative kinetic investigation into the nature of the interactions between PEP, Mn^{2+}, and FDP with YPK has been described (Mesecar & Nowak, 1997a), using the approach described by Reinhart (1983, 1985). The results of that investigation indicate that the divalent metal cation is responsible for directing the allosteric response of YPK to both PEP and FDP and for modulating the cooperative behavior of the enzyme. Very little direct interaction exists between the PEP and FDP sites in the absence of the metal. This result is captivating because "classical" descriptions of the regulation of pyruvate kinase (PK) explain the allosteric activation by FDP, the product of the phosphofructokinase reaction, as feed-forward activation of pyruvate kinase by increasing the affinity of PK for the substrate PEP. It is generally assumed that the PEP and FDP sites communicate with each other directly on the surface of the protein. It has not been previously recognized that the divalent metal plays an important role in the regulation of this complicated enzyme. Because of the significance of this result and

† Supported by a grant from the National Institutes of Health (DK 17049).

* Author to whom correspondence should be addressed.

‡ Present address: Department of Molecular and Cell Biology, University of California at Berkeley, Berkeley, CA 94596.

§ Recipient of a GAANNP fellowship from the United States Department of Education.

⊗ Abstract published in *Advance ACS Abstracts,* May 15, 1997.

[1] Abbreviations: PK, pyruvate kinase; YPK, yeast pyruvate kinase; ADP, adenosine 5′-diphosphate; PEP, phospho(enol)pyruvate; FDP, fructose 1,6-diphosphate; MES, 2-(*N*-morpholino)ethanesulfonic acid; YEPD, yeast extract peptone dextrose; DEAE, diethylaminoethyl; BME, β-mercaptoethanol; KP_i, potassium phosphate buffer; MWC, Monod, Wyman, Changeux model of allosteric control (Monod et al., 1965); KNF, Koshland, Nemethy, Filmer model of allosteric control (Koshland et al., 1966).

S0006-2960(96)02870-X CCC: $14.00

because of potential difficulties in interpreting kinetic parameters as thermodynamic parameters, we have initiated a thermodynamic investigation of the interactions of PEP, FDP, and Mn^{2+} with YPK using the approach described by Wyman (1948, 1964, 1965) and Weber (1972, 1975). These studies have been found to be complementary.

MATERIALS AND METHODS

Materials. *Saccharomyces cerevisiae* strain PYK1-5 (*a, ade1, leu1, met14, ura3, pyk1-5*), containing a YPK overexpression plasmid (pPYK101), was a generous gift from Dr. James Blair (University of Oklahoma). MES, potassium diphosphate, EDTA, the cyclohexylammonium salts of ADP, FDP and PEP, disodium NADH, sorbitol, lyticase (from *Arthobacter luteus*), DEAE cellulose (fibrous form 0.95 mequiv/g), and cellulose phosphate (fibrous form 1.2 mequiv/g) were obtained from Sigma. Ammonium sulfate was purchased from ICN biochemicals.

Pyruvate Kinase Assay. Yeast pyruvate kinase activity was measured by a continuous assay coupled to lactate dehydrogenase (Bücher & Pfleiderer, 1955). The change in absorbance at 340 nm due to oxidation of NADH was measured using either a Gilford Model 240, 250, or 260 thermostated spectrophotometer. The specific activity of the enzyme was measured during the purification as described in the previous paper (Mesecar & Nowak, 1997a). Purified enzyme has a specific activity between 230 and 310 units/mg at 24 °C. The concentration of purified YPK was determined by its absorbance at 280 nm using an extinction coefficient, ϵ_{280}, of 0.51 $(mg/mL)^{-1}$ for a 1 cm cell (Yun et al., 1976).

Purification of Recombinant Pyruvate Kinase. *Yeast Cell Growth and Lysis*. Six 10 mL aliquots of starter cultures were used to inoculate six 1 L YEPD cultures. The cultures were then incubated and shaken at 30 °C for 36−48 h. When the turbidity of each of the cultures at 600 nm reached 1.4−1.9, the yeast cells were harvested by centrifuging at 6000 rpm for 15 min. The supernatants were assayed for pyruvate kinase activity and discarded, and the wet weight of the yeast pellet was determined.

The pellets were suspended in 10 mL of lyticase buffer (1.2 M sorbitol, 20 mM BME, 5 mM EDTA, 10 mM potassium phosphate, pH 7.0) per gram of cells. A lyticase solution (1000 units/g of cells, in 10 mL of 10 mM KP_i buffer, pH 7.0) was then added to the suspension, and the mixture was incubated with gentle stirring for 2 h at 37 °C.

The resulting spheroplasts were centrifuged at 3000 rpm for 15 min, and the supernatant was removed and saved. The spheroplasts were then osmotically ruptured by addition of 10 mL of lysis buffer (1 mM KP_i, 5 mM EDTA, 5 mM BME) per gram of cells. The resulting cell debris was pelleted by centrifugation at 10000 rpm for 15 min. The supernatant was removed and saved, and the remaining pellet was resuspended in 5 mL of lysis buffer/g of cells. The cell debris was pelleted as before. The supernatants from each step were assayed for PK activity and protein content. All three supernatants were pooled, and the pH was adjusted to 7.0.

DEAE-Cellulose Batch Chromatography. One hundred and fifty grams of DEAE cellulose in 10 mM KP_i[1] buffer (5 mM EDTA, 5 mM BME, pH 7.0), previously precycled and equilibrated, was poured into a plastic Büchner funnel (diameter = 175 mm, height = 90 mm) that had two pieces of Whatman no. 1 filter paper serving as a frit. The Büchner funnel was attached to a 2 L side-arm flask that was connected to a vacuum. The pooled lysis fraction was gently poured onto the DEAE-cellulose. The solution was then carefully washed through the resin by applying a gentle vacuum so that foaming of the DEAE effluent was minimized. Once the lysis fraction had completely passed through the DEAE-cellulose, the resin was washed with 250 mL of 10 mM KP_i buffer. The DEAE effluent solution was then adjusted to pH 6.0 with 1 M HCl.

Phosphocellulose Batch Chromatography. One hundred and fifty grams of phosphocellulose in 10 mM potassium phosphate buffer (5 mM EDTA, 5 mM BME, pH 6.0), previously precycled and equilibrated, was carefully titrated into the DEAE effluent solution. The suspension was mixed by gently swirling the contents periodically over a 1 h time period. Since pyruvate kinase binds to phosphocellulose at pH 6.0, binding of YPK to the resin was checked over time by assaying for absence of activity in the supernatant. After a 1 h time period, less than 0.6% of the total activity remained unbound in the supernatant.

The unbound supernatant was poured off and discarded. The phosphocellulose slurry was then poured into an Ace Glass column (diameter = 40 mm, height = 460 mm) that was equipped with an on-line UV detector (ISCO) set at 280 nm. The resin was washed with 2 L of 10 mM KP_i buffer (25% glycerol, 5 mM EDTA, 5 mM BME, pH 6.0) at a flow rate of approximately 200 mL/h. The absorbance at 280 nm was less than 0.02.

Proteins were eluted from the column by a 4 L linear gradient from 0 to 0.6 M KCl in 10 mM KP_i buffer (25% glycerol, 5 mM EDTA, 5 mM BME, pH 6.0). Approximately 220 fractions were collected each having a volume of 17−18 mL. Fractions were assayed for protein and PK activity. The pH of fractions having greater than 150 units/mL PK activity was immediately adjusted to pH 6.2. Fractions having greater than 190 units/mL were pooled for further purification.

Ammonium Sulfate Backwashes. The pooled fractions from the phosphocellulose column were concentrated to greater than 10 mg of protein/mL using a 400 mL ultrafiltration cell (Amicon) equipped with a PM30 membrane. The concentrated protein was then dialyzed overnight against buffer (25% glycerol, 10 mM KP_i, 5 mM BME, 5 mM EDTA, pH 6.2) saturated in ammonium sulfate. The precipitated protein was centrifuged for 1 h at 15000 rpm in a 50 mL centrifuge tube, and the supernatant was removed and assayed for PK activity. The protein pellet was then washed with two, 40 mL aliquots of buffers (25% glycerol, 10 mM KP_i, 5 mM BME, 5 mM EDTA, pH 6.2) that were 56% (0.3568 g/mL), 54% (0.3435 g/mL), 48% (0.2985 g/mL), and 44% [0.2706 g $(NH_4)_2SO_4$/mL buffer] saturated in ammonium sulfate, respectively. The washes were performed in descending succession. The precipitated protein from each backwash was repelleted by centrifuging for 1 h at 15000 rpm. The supernatants were removed and assayed for pyruvate kinase activity and for protein concentration (absorbance at 280 nm). Supernatants that had specific activities greater than 200 units/mg were combined. The pooled backwashes were concentrated to greater than 10 mg of protein/mL using a 200 mL ultrafiltration cell

(Amicon) equipped with a PM10 membrane. The purified enzyme was then stored at 4 °C.

Steady-State Fluorescence Measurements. The steady-state intrinsic YPK fluorescence intensity was measured on an SLM model 8100 fluorimeter thermostated at 24 ± 1 °C. The excitation monochromator was a model MC400, and the emission monochromator was a model MC200. Emission spectra were recorded between 310 and 400 nm with a band width of 2 nm and a scan rate of 0.2 nm/s. Fluorescence titrations were performed by monitoring the change in fluorescence intensity at 334 nm with a band width of 2 nm. The excitation wavelength was 295 nm with a band width of 1 nm. Fluorescence titrations were performed by sequentially adding 1−10 μL aliquots of a concentrated ligand solution to 900 μL of a mixture containing MES (100 mM), pH 6.2, glycerol (5%), KCl (200 mM), YPK (0.05−0.07 mg/mL), and other ligands where specified. The percent fluorescence quenching, Q, was calculated from the following formula: $Q = [(F - F_o)/F_o]100$, where F is the fluorescence intensity of YPK in the presence of a ligand and F_o is the fluorescence intensity of YPK in the absence of a ligand. F was corrected for fluorescence intensity change due to dilution. Fluorescence titration data were fit to each of the following formulas:

$$Q = Q_{max}/(1 + K_D/[L]) \quad (1)$$

$$Q = Q_{max}/(1 + (K_D/[L])^{n_H}) \quad (2)$$

where L represents the variable ligand concentration, K_D is the dissociation constant for ligand L, Q_{max} is the percent maximal quenching, and n_H is the Hill coefficient. Equations 1 and 2 are analogous to the Michaelis−Menten and Hill equations, respectively.

Thermodynamic Treatment of the Data. The thermodynamic relationships that govern multiple ligand binding to proteins are based on the general relationships derived by Wyman (1948, 1964, 1965) and Weber (1972, 1975). Consider the binding of two ligands, M (Mn^{2+}) and S (PEP) to an enzyme E. The following equilibrium equations result:

$$E + S \rightarrow ES \quad (I)$$

$$E + M \rightarrow EM \quad (II)$$

$$ES + M \rightarrow ESM \quad (III)$$

$$EM + S \rightarrow EMS \quad (IV)$$

The standard free energy changes, or "unconditional free energies" of reactions I and II are designated $\Delta G°_S$ and $\Delta G°_M$, respectively. Reactions III and IV correspond to the binding of M when S is already bound and to the binding of S when M is already bound to E, respectively. The standard free energy changes of reactions III and IV are designated $\Delta G°_{M/S}$ and $\Delta G°_{S/M}$ and are called the "conditional free energies" since they presuppose the presence of another ligand. From the conservation of free energy and the principle of thermodynamic linkage, the total standard free energy change, $\Delta G°_T$, that results from the simultaneous binding of both S and M to E in forming the ESM complex is equal to the sum of the standard free energy changes for each step where

$$\Delta G°_T = \Delta G°_S + \Delta G°_{M/S} = \Delta G°_M + \Delta G°_{S/M} \quad (3)$$

The coupling free energy between the metal and substrate that binds to different sites on the enzyme, $\Delta G°_{SM}$, is equal to the difference between the sum of the unconditional free energies of binding of S and M and the standard free energy of formation of ESM:

$$\Delta G°_{SM} = (\Delta G°_S + \Delta G°_{M/S}) - (\Delta G°_S + \Delta G°_M)$$
$$= (\Delta G°_M + \Delta G°_{S/M}) - (\Delta G°_S + \Delta G°_M) \quad (4)$$

or

$$\Delta G°_{SM} = \Delta G°_{S/M} - \Delta G°_S = \Delta G°_{M/S} - \Delta G°_M \quad (5)$$

The value for $\Delta G°_{SM}$ may be greater than, less than, or equal to zero. When $\Delta G°_{SM} = 0$, there is independent binding of S and M to E and no mutual influence between their respective binding exists. If $\Delta G°_{SM}$ is positive, then the simultaneous binding of S and M to the enzyme is unfavorable, and the interaction between their sites is termed antagonistic. If $\Delta G°_{SM}$ is negative, then the simultaneous binding of S and M to E is favorable and their binding is termed cooperative.

A third ligand, or an allosteric effector F (FDP), when introduced into the complex, may influence the binding of S and/or M to the enzyme introducing new free energy terms $\Delta G°_{S/F}$ and $\Delta G°_{M/F}$ as well as $\Delta G°_F$. Ligand F may also act by altering the coupling free energy $\Delta G°_{SM}$ between the S and M sites indicating that $\Delta G°_{SM}$ is not equal to $\Delta G°_{SM/F}$. A coupling term also exists that represents the difference between the measured free energy change upon the simultaneous binding of all three ligands to E and that was calculated from the independent interaction of each ligand with free enzyme. The three ligand coupling term $\Delta G°_{SMF}$ is given by the following equation:

$$\Delta G°_{SMF} = (\Delta G°_S + \Delta G°_{M/S} + \Delta G°_{F/SM}) - (\Delta G°_S + \Delta G°_M + \Delta G°_F) \quad (6)$$

where $\Delta G°_{F/SM}$ is the free energy of binding for F when S and M are already bound to E. In addition to the conditional two ligand coupling term $\Delta G°_{SM/F}$, we also have the conditional two ligand coupling terms $\Delta G°_{MF/S}$ and $\Delta G°_{SF/M}$ and the unconditional two ligand coupling terms $\Delta G°_{MF}$ and $\Delta G°_{FS}$. The two ligand coupling terms are related by the following equations:

$$\Delta G°_{SM/F} = \Delta G°_{S/FM} - \Delta G°_{S/F} = \Delta G°_{M/SF} - \Delta G°_{M/F} \quad (7)$$

or

$$\Delta G°_{MF/S} = \Delta G°_{M/FS} - \Delta G°_{M/S} = \Delta G°_{F/SM} - \Delta G°_{F/S} \quad (8)$$

or

$$\Delta G°_{SF/M} = \Delta G°_{S/MF} - \Delta G°_{S/M} = \Delta G°_{F/SM} - \Delta G°_{F/M} \quad (9)$$

By combining eqs 4−9, the following relationship between the three ligand coupling term $\Delta G°_{SMF}$ and the two ligand coupling terms is established:

$$\Delta G^\circ_{SMF} = \Delta G^\circ_{MF/S} + \Delta G^\circ_{SF} + \Delta G^\circ_{SM} \quad (10)$$

$$= \Delta G^\circ_{SM/F} + \Delta G^\circ_{SF} + \Delta G^\circ_{MF}$$

$$= \Delta G^\circ_{SF/M} + \Delta G^\circ_{SM} + \Delta G^\circ_{MF}$$

From eqs 4−10, it is apparent that because of identities, all of the combinations of coupling free energies do not have to be measured to fully describe a three ligand coupled system. This is the advantage of using a thermodynamic linked-function analysis. Thus, by determining the equilibrium constants for a minimum number of five complexes, all of the two ligand coupling terms and the three ligand coupling terms may be calculated from the following relationship:

$$\Delta G^\circ = -RT \ln K \quad (11)$$

where R equals the gas constant, T equals absolute temperature, and K is equal to the reciprocal of the dissociation constant, K_D. Dissociation constants calculated from eq 1 ($n_H = 1$ or the zero cooperativity case) are the individual binding constants for the ligand to that site, and ΔG represents the intrinsic binding free energy. Dissociation constants calculated from eq 2 ($n_H \neq 1$ or the positive or negative cooperativity case) are the geometric means of the individual site dissociation constants for a dimer $K_D = (K_{D1}K_{D2})^{1/2}$, and for a tetramer, the dissociation constant is a complex function of both the intrinsic binding coefficients and the magnitude of the homotropic interactions. Therefore, it is most convenient to treat the $K_{0,5}$ value (concentration of ligand at half-maximal saturation) as the apparent K_D value making ΔG for a tetramer a measure of the average intrinsic free energy of the n successive additions of the ligand.[2]

Curve Fitting. Data were fit to the appropriate equations using the nonlinear least-squares fitting program EZ-FIT (Perella, 1988). The program was run on an IBM compatible 80386 computer equipped with a math coprocessor. The error in the fitted parameters is shown as error bars in graphs and was used as weighting factors in model fitting. The weighting factor used was 1/(error in parameter)^2.

RESULTS

Purification of Yeast Pyruvate Kinase. The results of the purification procedure for yeast pyruvate kinase are summarized in Table 1. Under optimal growth conditions, approximately 30% of the total soluble protein extracted from yeast is composed of YPK. Thus, pyruvate kinase is overexpressed in *S. cerevisiae* PYK1-5 containing the pPYK101 plasmid, consistent with the results of Burke et al. (1983). The overexpression of YPK can be induced by increasing concentrations of glucose (Mesecar, 1995).

A simple, rapid and reproducible purification procedure was developed for overexpressed YPK. The procedure utilized batch chromatographic procedures resulting in reduced purification time and large yields of highly purified YPK. From 90 g of wet weight of yeast, 370 mg of YPK, having a specific activity of 325 units/mg at 24 °C, was obtained. The enzyme was over 95% pure as judged by SDS−PAGE (data not shown). The percent yield of total PK activity from this procedure is comparable with other purification methods (Yun et al., 1976; Fell et al., 1974). The total yield of PK per gram of cells from the recombinant yeast is 10−50 times higher than the yields for wild-type PK reported in those previous studies.

Table 1: Purification Summary for Overexpressed Yeast Pyruvate Kinase

purification step	total units	total protein (mg)	specific activity (units/mg)	yield (%)	purification factor
lysis	304 700	3170	96	100	1
DEAE	210 200	1450	145	69	1.5
phosphocellulose	148 300	563	263	49	2.7
$(NH_4)_2SO_4$ backwash	110 400	371	298	36	3.1

Intrinsic Fluorescence Changes of YPK upon Ligand Binding. Yeast pyruvate kinase is a tetrameric enzyme that is composed of four identical subunits each having a polypeptide chain length of 500 residues. YPK is homologous to rabbit and cat muscle enzymes, both of which have had their three-dimensional structures solved by X-ray diffraction (Larsen et al., 1994; Allen & Muirhead, 1996).[3] Each subunit of pyruvate kinase is composed of four domains designated N, A, B, and C (Figure 1A). Domain N is the N-terminal segment, domain A is a α/β-barrel motif that contains the catalytic site, domain B sits above the catalytic site region, and domain C is located at the bottom of the α/β-barrel domain. There is a single tryptophan residue per subunit of YPK located at position 452, and this residue is highly conserved in all eukaryotic PKs. This conserved tryptophan is located in the first turn of the Cα5 helix in the C domain and is packed against a loop that connects two β-sheets, Cβ4 and Cβ5 (Figure 1B). The C domain is involved in the 1,3-intersubunit contact which is located between the Cα1 and Cα2 helixes of each subunit. It is proposed that this region may be involved in conferring the allosteric properties of the enzyme (Noguchi et al., 1986). Small conformational changes in either the Cα5 helix or the Cβ4 and Cβ5 sheets would be expected to perturb the environment of the tryptophan residue. Thus, if ligand binding to the enzyme induces a conformational change in this region, then a change in the tryptophan environment may result in a change in the intrinsic tryptophan fluorescence allowing this residue to be used as a probe for ligand binding and conformational changes.

The tryptophanyl fluorescence within pyruvate kinase has been used to monitor conformational changes upon ligand binding for both the muscle and yeast isozymes. In the case of the muscle enzyme, a quenching and change in polarization of the tryptophan fluorescence occurs upon the binding of KCl or $MnCl_2$ (Kayne & Price, 1972). The tryptophan fluorescence of the yeast enzyme is quenched upon the binding of FDP (Suelter, 1967; Kuczenski & Suelter, 1971). Monitoring the fluorescence change of this single tryptophan residue upon formation of various YPK−ligand complexes was performed in order to measure dissociation constants of ligands from various YPK complexes.

Fluorescence Spectra of YPK Complexes. The tryptophanyl fluorescence emission spectra of free YPK and of various

[2] For a more detailed discussion on the nature of ligand binding and interpretation of K_Ds in cooperative protein systems, consult Weber (1992).

[3] The X-ray crystallographic structure of the YPK−K^+−Mn^{2+}−phosphoglycolate−FDP complex is currently being solved in collaboration with Dr. Barry Stoddard, Fred Hutchinson Cancer Research Center.

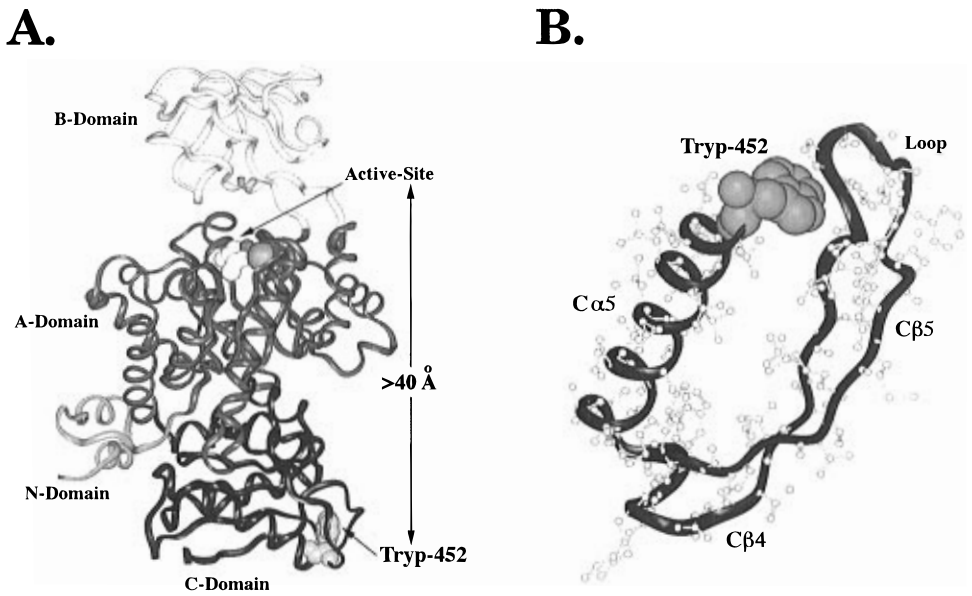

FIGURE 1: Location of the homologous tryptophan (Trp-452 in the YPK sequence) in the rabbit muscle enzyme (Larsen et al., 1994). (Panel A) Ribbon diagram of a single monomer of tetrameric pyruvate kinase indicating the location of the single tryptophan residue in relationship to the active site. Domains N, A, B, and C are labeled, respectively, and are shaded differently. Trp-452 is located in domain C, more than 40 Å away from the active site which is located between domains A and B. (Panel B) A detailed and expanded view of the single tryptophan environment located at the beginning of the Cα5 helix. The tryptophan side chain packs against the loop connecting the Cβ4 and Cβ5 beta sheet strands.

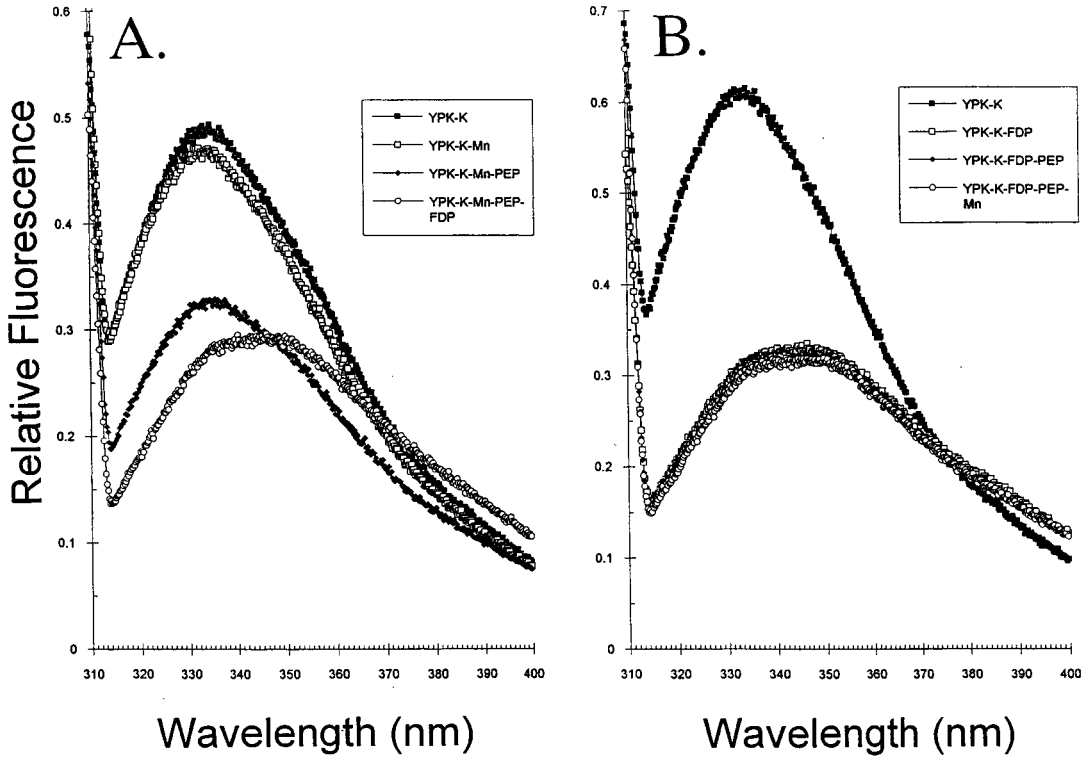

FIGURE 2: The intrinsic tryptophan fluorescence emission spectra of pyruvate kinase complexes excited at 295 nm. The YPK complexes indicated in the legend insert were formed by successively titrating free YPK to saturation with the indicated ligand. The spectra have been corrected for quenching due to dilution. The concentration of KCl was 200 mM, and all ligand concentrations are saturating. The final concentration of the ligands and the order of addition were as follows: (A) 0.056 mg/mL free YPK (■), 20 mM $MnCl_2$ (□), 1 mM PEP (◆), and 1 mM FDP (○); (B) 0.056 mg/mL free YPK (■), 2 mM FDP (□), 5 mM PEP (◆), and 1 mM $MnCl_2$ (○).

YPK complexes is shown in Figure 2A. The single tryptophan was selectively excited at 295 nm so that observed changes in fluorescence could be correlated to conformational changes in a specific localized area of YPK. Free pyruvate kinase in the presence of buffer and KCl has a tryptophan emission maximum at 334 nm. Upon saturation of YPK with Mn^{2+}, the emission maximum is shifted to the blue by 2 nm and the maximal fluorescence quenching obtained is 9%. Upon saturation of the YPK−Mn^{2+} complex with PEP, a small red shift of 2 nm occurs and the fluorescence quenching increases by 32%. Addition of FDP to the YPK−Mn^{2+}−PEP causes a large red shift of approximately 10 nm, a 19% decrease in the fluorescence intensity and a broadening of the spectra. It is clear from Figure 2A that the YPK−Mn^{2+}−PEP and the YPK−Mn^{2+}−PEP−FDP complexes have different conformations in terms of the environment

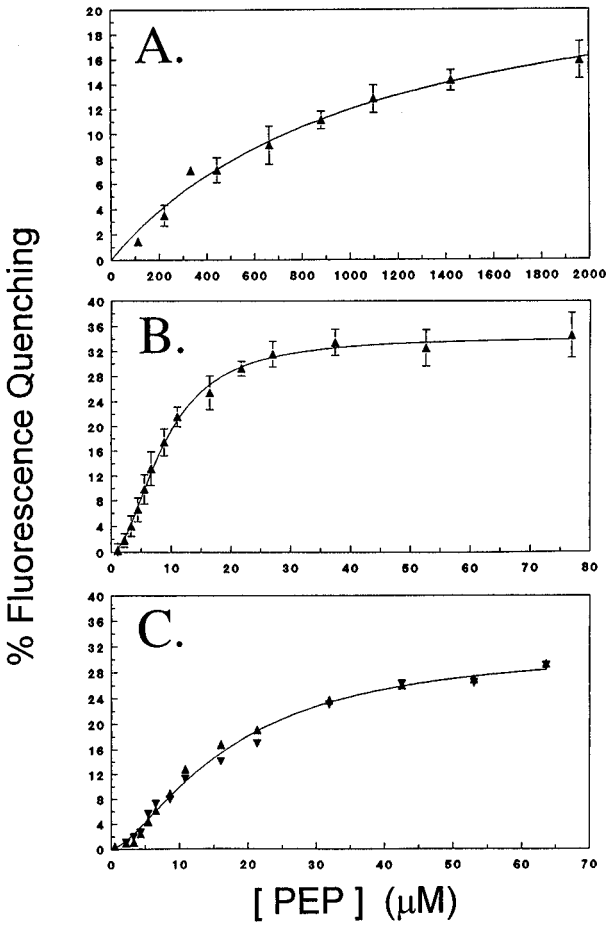

FIGURE 3: The binding of PEP to various yeast pyruvate kinase complexes as followed by intrinsic tryptophan fluorescence quenching. All complexes contain 200 mM KCl, and all nonvaried ligand concentrations are saturating. Error bars represent the standard deviation of triplicate experiments. The resulting best-fit parameters are summarized in Table 2. (A) The interaction of PEP with free YPK. The data were best-fit to eq 1. (B) The interaction of PEP with the YPK−K−Mn^{2+} complex with [Mn^{2+}] = 4 mM. The data were best-fit to eq 2. (C) The interaction of PEP with the YPK−K−Mn^{2+} complex with [Mn^{2+}] = 22 mM. The data were best-fit to eq 2. Results of duplicate experiments are shown. The curves are calculated giving a best-fit to the data.

around the tryptophan residue. Each of these complexes are formed in the presence of 0.2 M KCl.

Upon saturation of the free YPK complex with FDP, a 10 nm red shift occurs along with a 50% quenching of the fluorescence intensity (Figure 2B). The addition of both PEP and Mn^{2+} to the YPK−FDP complex causes no additional changes in the spectra. Thus, the environment of the tryptophan in the YPK−FDP, YPK−PEP−FDP, and YPK−Mn^{2+}−PEP−FDP complexes is approximately the same in terms of their steady-state fluorescence spectra. The ability to observe large changes in fluorescence intensity upon formation of various YPK complexes indicates that the measurements of ligand dissociation constants for some complexes is amenable by fluorescence.

Binding of PEP to YPK Complexes. All YPK complexes studied contained saturating levels (0.2 M) of K^+, and this complex is defined herein as the free enzyme. Titration of free YPK with PEP resulted in a significant quenching of the tryptophanyl fluorescence. A plot of percent fluorescence quenching versus PEP concentration is shown in Figure 3A. The response of free YPK to increasing concentrations of PEP was fit to eq 1, which describes a simple hyperbola. The resulting values for the dissociation constant (K_D) and Q_{max} are 1106 ± 187 μM and 25 ± 2%, respectively.

Figure 3B shows the data for the fluorescence response of YPK to PEP in the presence of 4 mM Mn^{2+}. The response of YPK to PEP under these conditions is sigmoidal. The data in Figure 3B was fit to eq 2, and the values calculated for K_D, Q_{max}, and n_H are 8.8 ± 0.3 μM, 34.5 ± 0.5%, and 2.0 ± 0.1, respectively. Figure 3C shows that increasing the concentration of Mn^{2+} to approximately 3 times its K_D value (7.2 mM, vide infra) causes an increase in the K_D of PEP to 16.7 ± 1.3 μM and a decrease in n_H to 1.5 ± 0.1. Q_{max} remains relatively unaffected by higher concentrations of Mn^{2+}. These results indicate that Mn^{2+} heterotropically induces homotropic cooperativity in PEP binding. Saturating concentrations of Mn^{2+} do not abolish the homotropic behavior of PEP binding. These results are consistent with the results of our kinetic studies (Mesecar & Nowak, 1997a). At lower concentrations of fixed Mn^{2+}, the values of n_H for PEP binding approach values of 1, and at higher concentrations of Mn^{2+} the values of n_H for PEP approach values near 2. Heterotropically induced homotropic cooperativity, as observed above, is to be distinguished from subsaturating heterotropic cooperativity. Under conditions of subsaturating heterotropic cooperativity, no cooperativity would be apparent in the PEP binding profile when [Mn^{2+}] = 0 or [Mn^{2+}] is saturating. Cooperativity will only be apparent when the concentration of Mn^{2+} is subsaturating and > 0 (Reinhart, 1988).

The interaction of PEP with YPK in the presence of saturating FDP could not be measured by steady-state fluorescence since no additional change in the intensity of the fluorescence emission spectra of the YPK−FDP or YPK−Mn^{2+}−FDP complexes could be measured upon the addition of PEP. Alternative direct binding methods for the measurement of the dissociation of PEP from the YPK−FDP and YPK−Mn^{2+}−FDP complexes were sought, but none were successful.[4] Kinetic studies indicate that the response of YPK to the binding of PEP, when YPK is saturated with FDP and Mn^{2+}, is hyperbolic (Mesecar & Nowak, 1997a). Thus, FDP heterotropically abolishes the homotropic binding of PEP to the YPK−FDP-Mn^{2+} complex. Our kinetic studies also indicate that as the concentration of free Mn^{2+} decreases and as the concentration of FDP increases, the values of the Hill coefficient for PEP approach 1. These data suggest that FDP abolishes the cooperative binding of PEP.

Binding of Mn^{2+} to YPK Complexes. The interaction of Mn^{2+} with free YPK and with YPK complexed with PEP was studied by steady-state fluorescence titrations. A plot of the percent fluorescence quenching of free YPK as a function of Mn^{2+} concentration is shown in Figure 4A. The fluorescence response of free YPK to Mn^{2+} follows a simple

[4] Equilibrium dialysis could not be used as a direct binding method since ^{14}C-PEP nonspecifically binds to the dialysis membrane. PEP also binds nonspecifically to a number of membranes and solid matrices including Amicon and Millipore ultrafiltration membranes, centrifuge filtration devices, as well as Sephadex gel exclusion resins (data not shown). A variety of pretreatment methods did not alleviate these problems. The difficulties arising with nonspecific PEP binding were also observed in other investigations (Waygood et al., 1976; Johannes & Hess, 1973; Nowak & Lee, 1977). The interaction of PEP to YPK−FDP complexes could not be reliably measured by direct binding methods.

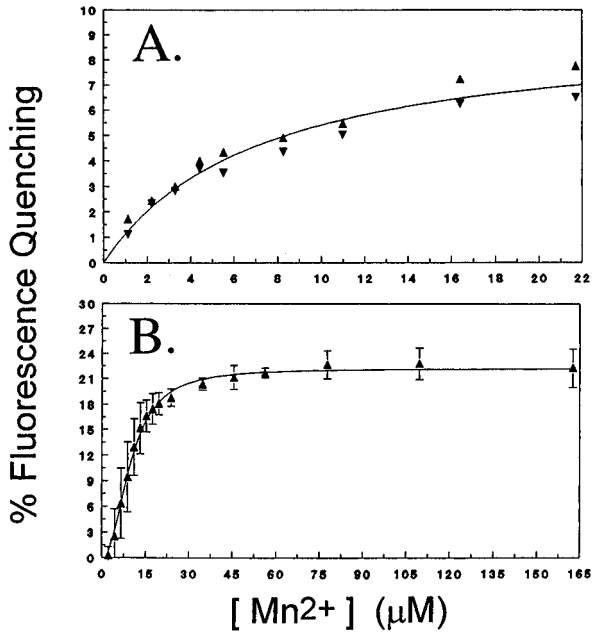

FIGURE 4: The binding of Mn^{2+} to various yeast pyruvate kinase complexes measured by intrinsic tryptophan fluorescence quenching. All complexes contain 200 mM KCl, and all nonvaried ligand concentrations are saturating. The resulting best-fit parameters are summarized in Table 2. Error bars represent the standard deviation of triplicate experiments. (A) The interaction of Mn^{2+} with free YPK. The data were best-fit to eq 1. The data represent duplicate experiments. (B) The interaction of Mn^{2+} with the YPK−K−PEP complex with [PEP] = 5 mM. The data were best-fit to eq 2.

rectangular hyperbola that can be fit to eq 1 with a dissociation constant of 7.2 ± 0.9 mM and a Q_{max} value of 9.3 ± 0.5%. The K_D value for Mn^{2+} binding to free YPK has been previously estimated from EPR studies to be > 1 mM (Fell et al., 1974; Nowak, T., unpublished data). The K_D value of Mn^{2+} to free YPK is approximately 130 times larger than the K_D value measured for Mn^{2+} binding to the rabbit muscle PK−K^+ complex (Nowak & Lee, 1977). This demonstrates that the nature of binding of Mn^{2+} to PK from both rabbit muscle and yeast apoenzymes is significantly different. One explanation for the difference is that the binding of Mn^{2+} to the yeast enzyme follows a preferred or an ordered binding path where PEP binds first followed by Mn^{2+}. Such a possibility has been suggested from the kinetic results by MacFarlane and Ainsworth (1972).

The binding of Mn^{2+} to the YPK−PEP complex, as monitored by a change in the intrinsic fluorescence, is shown in Figure 4B. Cooperative binding is observed, and the data were fit to eq 2. The resulting parameters are K_D = 9.9 ± 0.2 μM, Q_{max} = 22.2 ± 0.3%, and n_H = 2.23 ± 0.12. These values are in agreement with the values for K_M and n_H (14.9 ± 1.1 μM and 1.98 ± 0.28) determined by steady-state kinetics (Mesecar & Nowak, 1996a) and K_D and n_H (14.7 ± 2.5 μM and 1.87 ± 0.57) determined by EPR (Nowak, T., unpublished data). The binding of PEP to free YPK heterotropically induces homotropic cooperativity of Mn^{2+} binding. Since the binding of Mn^{2+} to YPK was measured in the presence of saturating PEP, subsaturating heterotropic cooperativity is not taking place.

The binding of Mn^{2+} to the YPK−FDP complexes could not be monitored by steady-state fluorescence for the same reason that the binding of PEP to these complexes could not be monitored. Mn^{2+} binding data obtained via EPR spectroscopy indicate that Mn^{2+} interacts with the YPK−PEP−FDP complex in a hyperbolic manner with a dissociation constant of approximately 2.5 μM and a binding stoichiometry of 3.2 moles of Mn^{2+}/mol of YPK (Nowak, T., unpublished data). Results from steady-state kinetics indicate that the response of YPK, in the presence of saturating FDP and PEP, to increasing concentrations of Mn^{2+} is hyperbolic (data not shown). The steady-state kinetic parameters for Mn^{2+} (calculated as Mn^{2+}_{free}) are K_M = 7.2 ± 0.5 μM, V_{max} = 60 ± 1 units/mg, and n_H = 1. These results indicate that FDP heterotropically abolishes the homotropic binding of Mn^{2+} to YPK.

Binding of FDP to YPK Complexes. The data in Figure 5A show that a large quenching of the intrinsic tryptophan fluorescence of free YPK is observed upon the binding of FDP and that the response of free YPK to FDP is sigmoidal. The data were fit to eq 2, and the resulting values for the parameters are K_D = 321 ± 7 μM, Q_{max} = 50.4 ± 0.9%, and n_H = 2.24 ± 0.09. The Hill coefficient indicates that FDP is binding to free YPK in a positive cooperative manner. In contrast, the hyperbolic binding isotherms for the interactions of Mn^{2+} and PEP with free YPK indicate that no cooperativity is observed. The sigmoidal response of free pyruvate kinase to FDP has also been observed with the enzyme isolated from *S. carlsbergenesis* (Johannes & Hess, 1973), *E. coli* (Waygood et al., 1976), and rat liver (El-Maghrabi et al., 1982).

The positive cooperative binding of FDP to YPK remains unchanged in the presence of saturating PEP. The resulting titration curve, Figure 5B, indicates that PEP does not change the cooperative nature of FDP binding and the resulting value of n_H is 2.27 ± 0.09. The dissociation constant for FDP decreases to 217 ± 5 μM, indicating that the PEP and FDP sites are weakly coupled, in agreement with our kinetic data (Mesecar & Nowak, 1997a).

The interaction of FDP with the YPK−Mn^{2+} complex is stronger than with the YPK or YPK−PEP complexes (Figure 5C). The dissociation constant for FDP decreases to 50.4 ± 0.9 μM. The FDP and Mn^{2+} binding sites appear to be more tightly coupled than the PEP and FDP sites. Interestingly, the homotropic cooperativity in FDP binding remains unchanged in the presence of Mn^{2+} since n_H has a value of 2.24 ± 0.09.

The Hill coefficient for FDP changes only when the enzyme is saturated with both PEP and Mn^{2+}. Figure 5D shows a plot of the fluorescence titration of YPK−PEP−Mn^{2+} by FDP. The resulting curve was best-fit to eq 2, and the resulting parameters K_D = 3.13 ± 0.14 μM, Q_{max} = 19.2 ± 0.3%, and n_H = 1.30 ± 0.07 indicate that FDP binds significantly more tightly to the ternary YPK−Mn^{2+}−PEP complex than to both of the respective binary complexes. The value of K_D and n_H are close to the kinetic parameters of K_a (7.8 ± 1.8 μM) and n_H (1.4 ± 0.4) determined from steady-state kinetics (Mesecar & Nowak, 1997a). The Hill coefficient indicates that the positive homotropic cooperativity in FDP binding is reduced but is not abolished in the presence of Mn^{2+} and PEP. The inability to totally suppress the cooperative nature of FDP binding upon saturation of the enzyme with both metal and substrate has also been observed with allosteric pyruvate kinases isolated from different sources (Johannes & Hess, 1973; Waygood et al., 1976; El-Maghrabi et al., 1982). The notion of a simple, two-state concerted allosteric transition mechanism, as

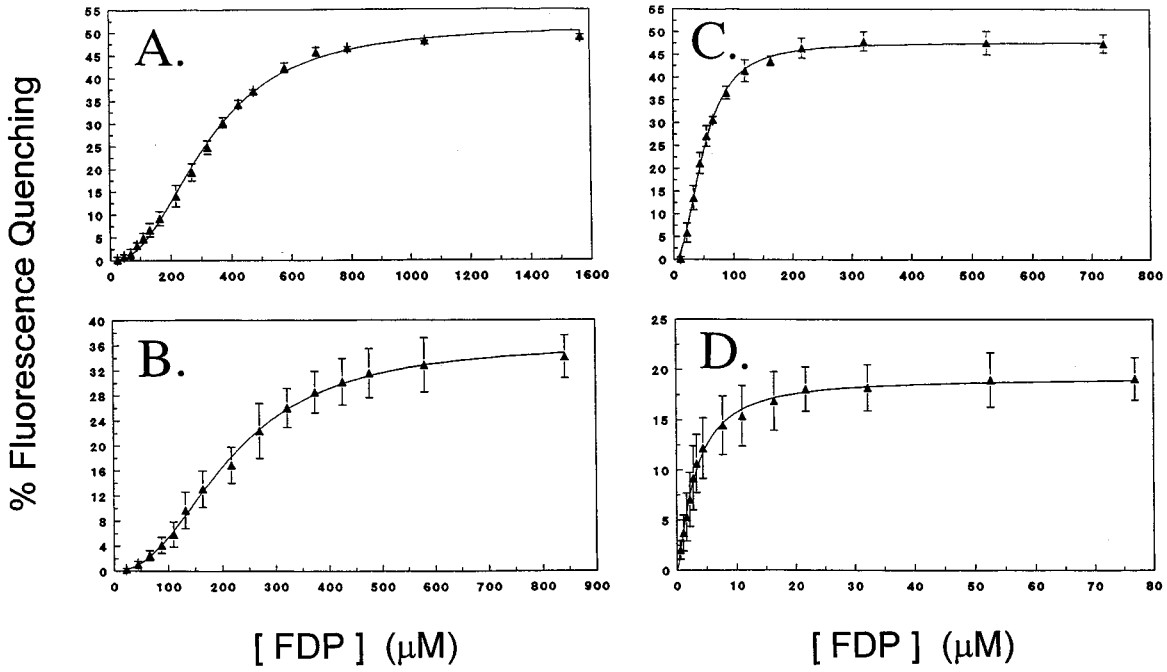

FIGURE 5: The binding of FDP to various yeast pyruvate kinase complexes measured by intrinsic tryptophan fluorescence quenching. All complexes contain 200 mM KCl, and all nonvaried ligand concentrations are saturating. Error bars represent the standard deviation of triplicate or quadruplicate experiments. (A) The interaction of FDP with free YPK. The data were best-fit to eq 2. (B) The interaction of FDP with the YPK−K−PEP complex with [PEP] = 5 mM. The data were best-fit to eq 2. (C) The interaction of FDP with the YPK−K−Mn^{2+} complex with [Mn^{2+}] = 4 mM. The data were best-fit to eq 2. (D) The interaction of FDP with the YPK−K−PEP−Mn^{2+} complex with [PEP] = 5 mM and [Mn^{2+}] = 4 mM. The data were best-fit to eq 2. The curves are calculated based on best-fit parameters. The resulting best-fit parameters are summarized in Table 2.

Table 2: Summary of Binding Constants for Yeast Pyruvate Kinase Complex Formation[a]

ligand	enzyme complex titrated	n_H	K_D (μM)	$\Delta G°$ (kcal/mol)[b]
PEP	YPK	1[c]	1106 ± 187	−4.02 ± 0.10
PEP	YPK−Mn^{2+} (4 mM)	1.98 ± 0.09	8.8 ± 0.3	−6.87 ± 0.02
PEP	YPK−Mn^{2+} (22 mM)	1.54 ± 0.11	16.7 ± 1.3	−6.49 ± 0.05
Mn^{2+}	YPK	1[c]	7160 ± 930	−2.92 ± 0.08
Mn^{2+}	YPK−PEP (5 mM)	2.23 ± 0.12	9.9 ± 0.2	−6.80 ± 0.02
Mn^{2+}	YPK−PEP (2 mM)[d]	1.87 ± 0.57	14.7 ± 2.5	−6.57 ± 0.10
Mn^{2+}	YPK−PEP (0.2 mM)−FDP (0.2 mM)[d]	1[c]	2.5 ± 0.1	−7.61 ± 0.02
FDP	YPK	2.38 ± 0.09	321 ± 7	−4.75 ± 0.02
FDP	YPK−PEP (5 mM)	2.27 ± 0.09	217 ± 6	−4.97 ± 0.01
FDP	YPK−Mn^{2+} (4 mM)	2.24 ± 0.09	50 ± 1	−5.84 ± 0.01
FDP	YPK−Mn^{2+} (4 mM)−PEP (1 mM)	1.30 ± 0.07	3.1 ± 0.1	−7.47 ± 0.03
FDP	YPK−Mn^{2+} (4 mM)−PEP (1 mM)[e]	1.50 ± 0.30	5.7 ± 0.3	−7.12 ± 0.03

[a] YPK is yeast pyruvate kinase in the presence of 200 mM KCl. The parameters were determined by steady-state fluorescence titrations unless otherwise indicated. [b] Calculated from eq 12 with T = 24 °C. [c] Equation 1 best-fit this data. [d] Determined from data obtained by EPR spectroscopy (T. Nowak, unpublished data). [e] Determined from data obtained by equilibrium dialysis (Mesecar & Nowak, 1997b).

proposed by Monod et al. (1965), for YPK must be discarded since this model would predict that the binding of FDP would be hyperbolic in the presence of saturating substrates.

A summary of the binding data measured for Mn^{2+}, PEP, and FDP to various respective complexes are given in Table 2.

DISCUSSION

The single tryptophan residue of yeast pyruvate kinase provides a unique probe for monitoring local conformational changes in the YPK structure. The observation of quenching of the intrinsic tryptophan fluorescence of YPK occurring upon the binding of PEP, ADP, Mn^{2+}, and FDP, allows for the measurement of thermodynamic dissociation constants for each of these ligands from various YPK complexes. The ability to measure a K_D value for the interaction of PEP, Mn^{2+}, and FDP with apoYPK suggests that random binding of these ligands may occur. MacFarlane and Ainsworth (1972) have suggested from the results of steady-state kinetic studies that ligand binding occurs in the order PEP, ADP, and metal. The discrepancies between the kinetic and direct binding studies may be explained by potential formation of various nonproductive or abortive complexes. The possibility of formation of a YPK−ADP complex is suggested from the results of both kinetic and direct binding studies (Mesecar & Nowak, 1997a). Collectively, our results suggest that a "preferred" ordered binding pathway is occurring with YPK, where either PEP or Mn^{2+} binds first forming the YPK−PEP−Mn^{2+} complex, followed by the addition of ADP. Also, metal binds more favorably when either PEP or ADP binds first. Further support for an ordered kinetic mechanism of YPK was proposed by Cottam et al. (1972) on the basis of both steady-state kinetic and direct binding studies.

The large quenching of the tryptophan fluorescence (52%) of YPK, induced by the binding of FDP, may result from a close proximity of the FDP binding site and the single tryptophan residue. Pereira (1990) observed little to no paramagnetic effects of YPK−Mn^{2+} on the ^{31}P nuclei of FDP, suggesting that the heterotropic effector site is distant from the Mn^{2+} binding site by more than 12 Å. Structures of pyruvate kinase determined thus far place the active-site and the homologous Trp-452 over 40 Å apart (Figure 1A). The FDP site would lie somewhere between the active site and Trp-452, possibly in the region of alternate splicing determined for the M1 and M2 pyruvate kinase isozymes (Noguchi et al., 1986).

The "extended sequential" model proposed for multiple ligand interactions with YPK is based on the results of kinetic studies and on the direct binding measurements described in this study (Mesecar & Nowak, 1997a,b). This model includes numerous liganded complexes, several of which are capable of catalytic turnover, and represents only the minimum number of ligation states necessary to explain the data collected for the interactions of PEP, Mn^{2+}, and FDP with YPK. The interactions of the other substrate (i.e., ADP) and allosteric ligands (K^+ and H^+) with YPK were not considered in the model, and any hysteretic transitions of YPK were excluded. Because of the numerous possible combinations of ligands with the enzyme and their various ligand binding pathways, the MWC (Monod et al., 1965) and KNF (Koshland et al., 1966) models for allosteric regulation were not expanded in this study to describe the allosteric regulation of YPK. The original MWC and KNF models were not developed to describe a protein that simultaneously interacts with three different ligands with each ligand involved in both homotropic and heterotropic interactions. Moreover, because a comprehensive mathematical description of a model analogous to the proposed extended sequential model has not been developed, the binding data for Mn^{2+}, PEP, and FDP was subjected to a thermodynamic linked-function analysis.

A thermodynamic linked-function analysis of ligand binding data for allosteric proteins has two major advantages over alternative approaches. First, the analysis is not based upon a priori mechanistic assumptions, but is based upon thermodynamic principles that treat the protein as a binding entity. The thermodynamic parameters involved have an absolute meaning.

Second, the thermodynamic approach stresses the importance of coupling parameters in describing allosteric behavior. It is the simultaneous binding of ligands to a protein that gives rise to the differential biophysical properties of that protein in solution. By condensing the multiple ligand couplings in terms of the equivalent two and three ligand coupling constant expressions, insight into the nature of the mechanistic origins of cooperative behavior can be obtained.

The standard free energies of interaction, $\Delta G°$, for the formation of various ligand−enzyme complexes were calculated from eq 11 and are summarized in Table 2. From these standard free energy changes, the standard two and three ligand coupling free energies were calculated from eqs 3−11 and are listed in Table 3. The two and three ligand coupling free energies calculated from binding data are all negative, indicating that the simultaneous binding of two or three ligands to YPK is more favorable than the binding of a single ligand to the apoenzyme.

Table 3: Comparison of Two and Three Ligand Standard Coupling Free Energies for the Interaction of YPK with PEP, Mn^{2+}, and FDP Determined by Direct Binding and by Kinetic Methods

coupling free energy between ligands (kcal/mol)	steady-state fluorescence[a]	steady-state kinetics[b]	rabbit muscle pyruvate kinase[c]
ΔG_{Mn-PEP}	-3.88 ± 0.08	-2.75 ± 0.36	-3.13 ± 0.08
	-2.85 ± 0.10[d]		
	-2.47 ± 0.11[e]		
ΔG_{Mn-FDP}	-1.09 ± 0.02	-1.77 ± 0.12	
$\Delta G_{PEP-FDP}$	-0.22 ± 0.03	0	
$\Delta G_{Mn-PEP-FDP}$	-6.60 ± 0.09	-4.22 ± 0.07	

[a] Calculated from eqs 3−10 from data described in this study. [b] Calculated from kinetic data taken from Mesecar and Nowak (1997a). [c] Data taken from Nowak and Lee (1972). [d] Calculated from PEP titration data in the presence of 4 mM Mn^{2+}. [e] Calculated from PEP titration data in the presence of 22 mM Mn^{2+}.

The coupling free energy for formation of the ternary YPK−Mn^{2+}−PEP complex, $\Delta G°_{SM}$, was calculated using eq 4. The values for $\Delta G°_{SM}$ are -3.88 ± 0.08 and -2.85 ± 0.10 kcal/mol. These values were calculated from different sets of experiments according to eq 4:

$$\Delta G°_{SM} = (\Delta G°_{S} + \Delta G°_{M/S}) - (\Delta G°_{S} + \Delta G°_{M}) = -2.85 \pm 0.10 \text{ kcal/mol}$$

$$= (\Delta G°_{M} + \Delta G°_{S/M}) - (\Delta G°_{S} + \Delta G°_{M}) = -3.88 \pm 0.08 \text{ kcal/mol}$$

where $\Delta G°_{S}$ = the unconditional free energy of binding of PEP and $\Delta G°_{M}$ = the unconditional free energy of binding of Mn^{2+} to free YPK, respectively; $\Delta G°_{M/S}$ is the conditional free energy of binding of Mn^{2+} to the YPK−PEP complex and $\Delta G°_{S/M}$ is the conditional free energy of binding of PEP to the YPK−Mn^{2+} complex. The coupling free energies indicate that formation of the ternary YPK−PEP−Mn^{2+} complex is favored over formation of the binary YPK−PEP and YPK−Mn^{2+} complexes by -2.85 ± 0.10 to -3.88 ± 0.08 kcal/mol. These two values for $\Delta G°_{SM}$ demonstrate a large reciprocal cooperative effect between Mn^{2+} and PEP as predicted by the principles of thermodynamic linkage is represented by eq 5. The inequality between these two calculations is most probably due to the uncertainty of the dissociation constant for Mn^{2+} from the YPK−Mn^{2+} complex. The high levels of Mn^{2+} (22 mM) needed to saturate the enzyme may increase the ionic strength to a level that interferes with the determination of an accurate K_D. High levels of Mn^{2+} have been shown to decrease the activity of the enzyme as well as cause an increase in the dissociation constant of PEP (Figure 3C). Thus, the value of −3.88 kcal/mol may be more accurate than the other two values listed for ΔG_{Mn-PEP}, since it was calculated from the K_D of PEP and the K_D of Mn^{2+} in the presence of saturating PEP, values more reliably determined. An alternate explanation for the inequality in $\Delta G°$ values would be that two different E−PEP−Mn^{2+} complexes are being formed depending upon the path of formation. This is considered unlikely because the titrations were performed under equilibrium conditions. The value of −3.88 kcal/mol corresponds closely to the value of −3.13 kcal/mol determined for the coupling between PEP and Mn^{2+} with the rabbit muscle enzyme (Nowak & Lee, 1977) analyzed by the methods of Weber (1972, 1975).

The large, negative Mn^{2+}−PEP coupling free energy indicates that strong cooperative interactions are taking place

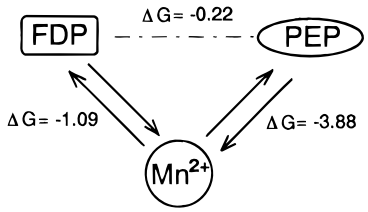

FIGURE 6: Allosteric relay mechanism of yeast pyruvate kinase. This three ligand heterotropic coupling model illustrates the mechanism by which FDP influences the binding of PEP and vice versa. FDP and PEP positively influence the binding of each other via the enzyme bound metal. Little direct interaction between the PEP and FDP sites exists. The coupling free energies are given in kilocalories per mole.

between these ligands when bound to YPK. Weber (1975) has predicted that most cooperative interactions will not exceed ±2 kcal/mol. Thus, the value of −3.88 kcal/mol is large when compared to this predicted value and to other two ligand coupling free energies determined for different proteins (Weber, 1975). One explanation for the large value of ΔG_{Mn-PEP} is that a direct electrostatic interaction between PEP and Mn^{2+} exists. The interaction of the phosphate group of PEP with Mn^{2+} has been suggested by a number of indirect studies (Nowak & Mildvan, 1972b; Nowak, 1978; Muirhead et al., 1987; Tipton et al., 1989; Tan et al., 1993). No conclusive evidence for a first coordination sphere interaction between PEP and Mn^{2+} has been provided to date. The nearly equivalent values of ΔG_{Mn-PEP} for both the yeast and rabbit muscle enzymes indicate that the path to formation of the E−Mn^{2+}−PEP complexes may occur by the same mechanism.

The coupling free energy of interaction between PEP and FDP ($\Delta G_{FDP-PEP}$) is weak at -0.22 ± 0.03 kcal/mol. This is surprising considering that numerous studies with allosteric pyruvate kinase from many sources suggest that the PEP and FDP sites are tightly coupled and that this value is large. These studies, however, have concentrated on the allosteric interactions of PEP and FDP with the enzyme in the presence of metal. No consideration was given to the coupling between the metal site with both the PEP and FDP sites. Our observation of weak coupling between PEP and FDP is further supported by the results of our kinetic studies where the value for $\Delta G_{FDP-PEP}$ was found to be close to zero, indicating that very little kinetic coupling is taking place (Mesecar & Nowak, 1997a).

The coupling between the FDP and PEP sites is accomplished through the enzyme bound metal (see model depicted in Figure 6). The value of $\Delta G_{Mn-FDP} = -1.09$ kcal/mol indicates that the FDP and Mn^{2+} sites are strongly coupled. Since the coupling between the Mn^{2+} and PEP is also strongly coupled, the following sequence is proposed. FDP increases the affinity of YPK for Mn^{2+}. Upon binding of Mn^{2+}, the affinity of the enzyme for PEP is increased. The converse, that PEP positively influences the binding of Mn^{2+} which then positively influences the binding of FDP, can also occur. The binding of either PEP or FDP in the absence of metal has little influence of the binding of the other ligand to its site. Thus, the allosteric communication between the PEP and FDP sites occurs via a relay through the activating divalent metal.

The resulting three ligand coupling free energy for the simultaneous binding of PEP, FDP, and Mn^{2+} is -6.60 ± 0.09 kcal/mol. This large, negative coupling free energy value indicates that formation of the YPK−Mn^{2+}−PEP−FDP complex is strongly favored over the formation of the other complexes (e.g., YPK−Mn^{2+}, YPK−PEP, YPK−FDP, YPK−Mn^{2+}−PEP, YPK−Mn^{2+}−FDP, and YPK−PEP−FDP). This coupling free energy value is one of the largest ever published for an allosteric enzyme and reveals an important thermodynamic driving force for the allosteric regulation of pyruvate kinase and hence regulation of the glycolytic pathway.

The results of this physical study strongly support the results of our kinetic analysis (Mesecar & Nowak, 1997a). Both studies used a thermodynamic linked-function approach in analyzing the experimental data. The power of such an approach was realized in the discovery that the enzyme-bound metal plays a central role in modulating the allosteric behavior of yeast pyruvate kinase. Although the absolute values of the thermodynamic parameters were slightly different in each study, interpretation of their possible biophysical origins yield the same conclusions. Any discrepancies could be explained by applying the principles of thermodynamic coupling to the additional ligands (e.g., ADP) that form the kinetically active complexes. The thermodynamically linked-function analysis with yeast pyruvate kinase best describes the pathway of multiple ligand interactions during allosteric activation and is the favored model in contrast to the conventional MWC and KNF models (Monod et al., 1965; Koshland et al., 1966).

REFERENCES

Allen, S. C., & Muirhead, H. (1996) *Acta Crystallogr. D52*, 499−504.

Bücher. T., & Pfleiderer, G. (1955) *Methods Enzymol. 1*, 435−440.

Burke, R. L., Tekamp-Olson, P., & Najarian, R. (1983) *J. Biol. Chem. 258*, 2193−2201.

Cottam, G. L., Mildvan, A. S., Hunsley, J. R., & Suelter, C. H. (1972) *J. Biol. Chem. 247*, 3802−3809.

El-Maghrabi, M. R., Claus, T. H., McGrane, M. M., & Pilkis, S. J. (1982) *J. Biol. Chem. 257*, 233−240.

Fell, D. A., Liddle, P. F., & Peacocke, A. R. (1974) *Biochem. J. 139*, 665−675.

Johannes, K.-J., & Hess, B. (1973) *J. Mol. Biol. 76*, 181−205.

Kayne, F. J., & Price, N. C. (1972) *Biochemistry 11*, 4415−4420.

Koshland, D. E., Nemethy, G., & Filmer, D. (1966) *Biochemistry 5*, 365−385.

Kuczenski, R. T., & Suelter, C. H. (1971) *Biochemistry 10*, 2862−2866.

Larsen, T. M., Laughlin, T., Holden, H. M., Rayment, I., & Reed, G. H. (1994) *Biochemistry 33*, 6301−6309.

Macfarlane, N., & Ainsworth, S. (1972) *Biochem. J. 129*, 1035−1047.

Mesecar, A. D. (1995) Ph.D. Dissertation, University of Notre Dame.

Mesecar, A. D., & Nowak, T. (1997a) *Biochemistry 36*, 6792−6802.

Mesecar, A. D., & Nowak, T. (1997b) *Biochemistry* (submitted for publication).

Monod, J., Wyman, J., & Changeux, J. (1965) *J. Mol. Biol. 12*, 88−118.

Noguchi, T., Inoue, H., & Tanaka, T. (1986) *J. Biol. Chem. 261*, 13807−13812.

Nowak, T. (1978) *Arch. Biochem. Biophys. 186*, 343−350.

Nowak, T., & Lee, M. J. (1977) *Biochemistry 16*, 1343−1350.

Nowak, T., & Mildvan A. S. (1972) *Biochemistry 11*, 2819−2828.

Pereira, M. A. P. (1990) Ph.D. Dissertation, University of Notre Dame.

Perrella, F. W. (1988) *Anal. Biochem. 174*, 437−447.

Reinhart, G. D. (1983) *Arch. Biochem. Biophys. 224*, 389−401.
Reinhart, G. D. (1985) *Biochemistry 24*, 7166−7172.
Reinhart, G. D. (1988) *Biophys. Chem. 30*, 159−172.
Suelter, C. H. (1967) *Biochemistry 6*, 418−423.
Tan, X., Poyner, R., Reed, G. H., & Scholes, C. P. (1993) *Biochemistry 32*, 7799−7810.
Tipton, P. A., McCracken, J., Cornelius, J. B., & Peisach, J. (1989) *Biochemistry 28*, 5720−5728.
Waygood, E. B., Mort, J. S., & Sanwal, B. D. (1976) *Biochemistry 15*, 277−282.
Weber, G. (1972) *Biochemistry 11*, 864−878.
Weber, G. (1975) *Adv. Protein Chem. 29*, 1−83.
Weber, G. (1992) *Protein Interactions*, pp 31−102, Chapman and Hall, New York.
Wyman, J. (1948) *Adv. Protein Chem. 4*, 410−531.
Wyman, J. (1964) *Adv. Protein Chem. 19*, 224−286.
Wyman, J. (1965) *J. Mol. Biol. 11*, 631−644.
Yun, S.-L., & Suelter, C. H. (1976) *J. Biol. Chem. 251*, 124−128.

BI962870S